

# Membrane flow patterns in multicomponent giant vesicles induced by alternating electric fields†

Margarita Staykova, Reinhard Lipowsky and Rumiana Dimova\*

Received 11th July 2008, Accepted 27th August 2008

First published as an Advance Article on the web 10th September 2008

DOI: 10.1039/b811876k

**Alternating electric (AC) fields induce circular patterns of lipid transport in membranes of giant vesicles. The flow is visualized by fluorescently labelled lipid domains.**

Electric fields induce various electrokinetic phenomena, which have found wide application in micro- and nano-technologies in the past decade. Electro-neutral particles (droplets, bubbles, lipid vesicles, solid beads) suspended in a medium of different polarizability acquire charge at their surfaces when exposed to electric fields. The interaction of the fields with the surface charges may result in particle kinetics, electro-osmotic fluid flow or a combination of both.<sup>1</sup>

Particle kinetics in electric fields arise from the interaction of the field with the field-induced dipole moment. Depending on the field geometry, freely suspended particles may translate, orient, rotate, deform, *etc.* These kinetic phenomena are widely used in biology and biotechnology as methods for cell or membrane characterization<sup>2</sup> and micro-manipulation.<sup>3</sup>

Electro-osmotic flows in the vicinity of polarizable objects are driven by the displacement of the free induced surface charges by the lateral component of the electric field. This phenomenon has been termed “induced-charge electro-osmosis” (ICEO)<sup>1</sup> and has drawn significant attention because of its vast application potential in microfluidics. ICEO has been reported and theoretically interpreted for the first time by Taylor in relation to the deformation of a droplet in a homogeneous steady electric field.<sup>4</sup> The flow outside the drop is symmetric on both sides facing the electrodes and is directed from the poles (the points nearest to the electrodes) to the equator. A similar flow pattern has been theoretically predicted for solid polarizable particles in AC fields.<sup>5</sup> More recently, external fluid flows have been studied for various geometries and conditions<sup>6</sup> but, to our knowledge, no experimental or theoretical studies on ICEO effects on lipid membranes have been pursued. Here, we report electro-osmotic lipid flow patterns induced by AC fields. We used giant vesicles, tens of micrometres in size, which are very suitable for direct microscopy observation of the influence of electric fields on membranes.<sup>2c</sup>

Lipid vesicles provide biomimetic models for cell membranes and have many biotechnological applications, *e.g.* as drug delivery systems, micro-reactors, *etc.* Since many techniques for cell manipulation, gene therapies and cancer treatment use electric fields as an external perturbation, it is important to understand the nature of

their effect on the membrane at the molecular level. Here, we implement fluorescent markers to visualize the flow patterns of the lipid movement within the membrane of a vesicle subjected to an AC field.

The behaviour of lipid vesicles in AC fields is determined to a large extent by the specific electric and mechanical properties of their membranes. The lipid membrane can be considered as a thin fluid layer hydrophobically confined at the surface of the vesicle. At low field frequencies the membrane behaves as an electric insulator between the inner and the outer electrolyte solutions. Charges accumulate on both membrane interfaces and the membrane is capacitively charged. At higher frequencies (*e.g.* above 1 kHz), the membrane capacitor becomes short-circuited and the induced surface charge density depends solely on the conductivities of the inner and outer vesicle media. Hydrodynamically, the membrane behaves as a two-dimensional incompressible fluid. To keep the surface area constant the lipid bilayer develops tension under forcing. Under homogeneous electric fields, an axially symmetric gradient in the membrane tension builds up, which effectively counterbalances the lateral component of the electric stress; see the ESI.† As a result, an electro-osmotic membrane flow in lipid vesicles is not expected.<sup>7</sup> However, in most chambers and conditions used for electric manipulation, vesicles, cells or other particles are located close to the chamber bottom between the electrodes, or among other cells or vesicles, or in the immediate vicinity of an electrode,<sup>8</sup> thus experiencing an inhomogeneous electric field. This inhomogeneity is even more pronounced in chambers for micro-manipulation where the electrodes are imprinted on a solid substrate.<sup>3b</sup> In this study, we show for the first time that even weakly inhomogeneous AC fields may induce a pronounced membrane flow in giant lipid vesicles.

We prepared giant lipid vesicles from dioleoylphosphatidylcholine (DOPC), dipalmitoylphosphatidylcholine (DPPC) and cholesterol (Chol) in molar ratios of 5.33 : 2.66 : 2, 2.66 : 5.33 : 2 or 4.8 : 3.2 : 2 DOPC : DPPC : Chol, using the electroformation method,<sup>9</sup> see the ESI.† A small fraction of *N*-(lyssamine rhodamine B sulfonyl)-dipalmitoylphosphatidylethanolamine (Rh-DPPE) (0.1 molar%) was added to the lipids for fluorescence microscopy observation. The vesicles were prepared in 0.01 to 0.1 M sucrose and subsequently diluted in isotonic glucose solution to prevent osmotic stress and to make them sediment to the bottom of the observation chamber. Up to about 3 mM NaCl was added to the glucose solution to adjust the vesicles' external conductivity. The internal conductivity was always in the range 2–5  $\mu\text{S cm}^{-1}$ , whereas the external one was varied between 2–5 and 300  $\mu\text{S cm}^{-1}$ . At room temperature, the ternary lipid mixture (with the above-mentioned composition) spontaneously separates in liquid-ordered ( $l_o$ ) and liquid-disordered ( $l_d$ ) phases, leading to the formation of  $l_o$  and  $l_d$  domains on the vesicles.<sup>10</sup>

Max Planck Institute of Colloids and Interfaces, Science Park Golm, 14424 Potsdam, Germany. E-mail: Rumiana.Dimova@mpikg.mpg.de; Fax: +49 331 567 9615; Tel: +49 331 567 9612

† Electronic supplementary information (ESI) available: Vesicle preparation procedure, numerical calculations and confocal microscopy movies of domain motion. See DOI: 10.1039/b811876k

Rh-DPPE preferentially partitions in the  $l_d$  domains. The ternary lipid composition and the temperature conditions determine the size of the domains. An optimal condition for our observation was provided by many small  $l_o$  domains, appearing as dark circular patches of 5–10  $\mu\text{m}$  diameter on a red background. The lipid domains turned out to be very suitable markers for studying membrane fluid dynamics induced by different stresses such as electric, hydrodynamic (e.g. shear flow), mechanic, etc.

The vesicles were exposed to AC fields of moderate field strengths (100–500  $\text{V cm}^{-1}$ ) and intermediate frequencies of 10 kHz to 20 MHz. The working chamber consists of two parallel cylindrical electrodes, 200  $\mu\text{m}$  in diameter, at a distance of 500  $\mu\text{m}$ . The distance of the electrodes from the bottom of the chamber, a glass surface, is ca. 2–5  $\mu\text{m}$ . Because of sedimentation, the vesicles are exposed to the field close to the bottom of the chamber. The observations were done with a confocal microscope at various focal planes across the vesicles, whereby the pinhole was widely open to allow for a large scan depth, see the ESI.† Appropriate for observation are single spherical vesicles located in the middle between the electrodes, with diameters between 70 and 150  $\mu\text{m}$ .

When the vesicles were exposed to AC fields, we observed some familiar electrokinetic phenomena. Under the conditions of our experiments, the vesicles experience negative dielectrophoresis, manifested as repulsion from the high field intensity regions, i.e. from the electrodes and the solid glass substrate. At the same time they deform, assuming an oblate shape as previously reported.<sup>2,11</sup> In addition, an interesting new phenomenon is observed, namely circular lipid flow patterns within the vesicle membrane.

The membrane flow is studied by following the motion of the lipid domains on the vesicle. Fig. 1 provides snapshots of this motion on the top and bottom vesicle parts, as well as schematic illustrations of the flow lines; movies showing the domain displacement are available in the ESI.† The flow velocity reaches about 30  $\mu\text{m s}^{-1}$  corresponding to laminar flows. It depends on the field conditions and on the location within the vesicle surface. In all experiments, the lipid transport is faster at the bottom part of the vesicle (closer to the glass).

The lipid dynamics on the vesicle surface is organized in four symmetric quadrants, each extending from the lower to the top part of the vesicle as illustrated in Fig. 1f. The motion follows concentric closed trajectories with the highest velocity at the periphery of each quadrant and at the vesicle bottom. Towards the quadrant centres, the velocity decreases creating stagnation points, where the motion stops. Note that these points appear slightly below the middle plane of the vesicle. For a vesicle with a radius of 75  $\mu\text{m}$ , the time period, during which a domain completes a full cycle of its trajectory, varies between about 10 s when located close to a quadrant centre, and 90 s when in the quadrant periphery. Additionally, there are two other stagnation points at the top and the bottom of the vesicle, where membrane motion is slowed down by the balance of oppositely directed forces. For smaller vesicles with diameters less than 60  $\mu\text{m}$ , the lipid flow does not fully extend to the upper hemisphere and the stagnation points in the quadrants are located even closer to the vesicle bottom.

We have further attempted to characterize the dependence of the lipid transport on the field parameters and the media properties. At higher field strength the motion is faster. At the same time however,

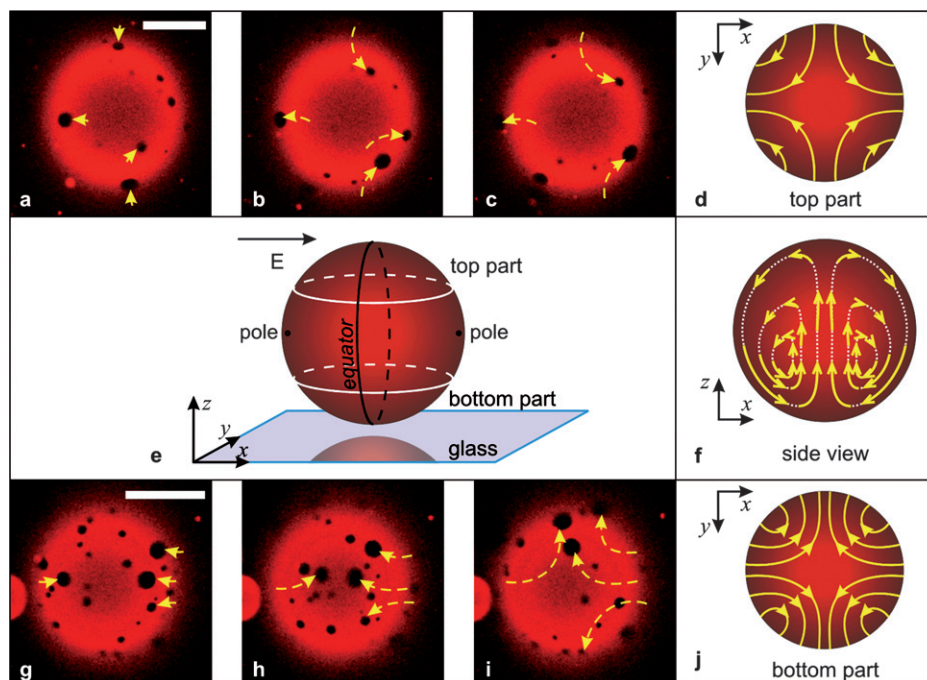


**Fig. 1** Confocal micrographs illustrating the membrane flow on the top (a–c) and bottom (g–i) parts of a giant vesicle ( $\sim 150 \mu\text{m}$  in diameter) induced by an AC field (360  $\text{V cm}^{-1}$ , 80 KHz), at external conductivity of 250  $\mu\text{S cm}^{-1}$ . The vesicle was prepared from a mixture of 4.8 : 3.2 : 2 DOPC : DPPC : Chol. The time between the consecutive snapshots is approximately 1.3 s for a–c and 6.5 s for g–i. The yellow dashed arrows indicate the trajectories of selected domains. The scale bars correspond to 50  $\mu\text{m}$ . The vesicle is located close to the bottom of the observation chamber as illustrated in (e), where the vesicle top and bottom parts, the poles and the equator as well as the field direction are indicated. The top, side and bottom view of the flow lines are sketched in (d), (f) and (j), respectively. The length of the arrows in (f) roughly corresponds to the flow velocity.

the negative dielectrophoretic force lifting the vesicles away from the glass substrate increases. The latter effect depends on the vesicle weight. For lighter vesicles, containing 0.01 M sucrose solution, the lipid motion in the membrane at first increases with increasing field strength and afterwards gradually decreases as they drift away from the bottom of the chamber. When the vesicles are far away from the glass substrate, the field is more homogeneous and the membrane motion may terminate completely even though the vesicle deformation is preserved. Vesicles with diameters between 70 and 150  $\mu\text{m}$ , containing 0.1 M sucrose, are heavy and are not lifted significantly for fields up to 400  $\text{V cm}^{-1}$ . The lipid flow is also enhanced by the external conductivity whereas it is very slow in salt-free external media.

Interesting behaviour was observed when the field frequency was varied; see the ESI.† At frequencies lower than about 1 MHz, the motion in the circular trajectories is directed downwards past the poles and upwards along the equator as sketched on Fig. 1f. With increasing frequencies the velocity of the motion gradually decreases and reverses its direction at around 3–5 MHz.

In order to get some insight into the onset of the membrane flow, we calculate the tangential force arising from the inhomogeneous electric field. For this purpose, we use a commercially available modelling package COMSOL (Multiphysics, Germany). Since the frequencies used in the experiments were well above 1 kHz and the internal solution has a very low conductivity, the induced charges arise from the external solution. Thus, we can use with good approximation the equivalent body model; for details see ESI.† According to it, the vesicle can be represented as a homogeneous spherical object with an effective permittivity and conductivity.<sup>12</sup> Fig. 2 presents the calculated distribution of the electric field around a vesicle at a frequency of 100 kHz; see the ESI† for details on the model parameters. The field strength exhibits minima at the vesicle poles and higher values at the equator. In addition, the vicinity of the glass causes asymmetric field distribution on the surface of the vesicle. The field is much higher at the lower region facing the glass than at the vesicle top. Such field distribution agrees well with our experimental findings for oblate deformation (enhanced electric pressure at the poles) and negative dielectrophoresis (high field strength at the bottom part pushes the vesicle upwards). Note that the out-of-sphere deformation of the vesicle is not taken into account in the calculations

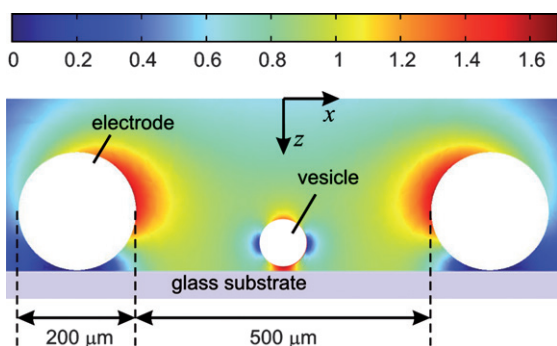


**Fig. 2** Electric field distribution at 100 kHz in a cross section of the chamber, passing through the centre of the vesicle. The vesicle is 40  $\mu\text{m}$  in radius and is located at 8  $\mu\text{m}$  above the glass. The media conductivity is 300  $\mu\text{S cm}^{-1}$ . The field inside the vesicle is not calculated. The data are rescaled with the strength of a field, which would be induced between two parallel planar electrodes at a distance of 500  $\mu\text{m}$ .

since it is relatively small and does not influence the results qualitatively.

Given the field distribution, we calculate the lateral electric stress (surface force density) on the membrane as the product of the field-induced free charge density at the vesicle surface and the tangential component of the electric field.<sup>4</sup> In homogeneous fields (electrodes and vesicle located high above the chamber bottom), the lateral stress distribution is axially symmetric; see the ESI.† It exhibits minima at the poles (zero tangential electric field) and at the equator (minimum induced free charge). The maxima are located at  $\theta = \pm\pi/4$ , where  $\theta$  is the angle between the radial vector of the vesicle and the field vector. The membrane tension adapts to the symmetric lateral stress. As a result no lipid flow is expected as observed for vesicles far away from the solid substrate.

The inhomogeneous electric field distribution for vesicles close to the glass (and generally in chambers for micro-manipulation) breaks the symmetry in the electric stress distribution between the lower and the upper hemispheres of the vesicle; see Fig. 3. Overall, the vesicle experiences significant stress at  $\theta = \pm\pi/4$ , as in the homogeneous case, but it is additionally enhanced in the vicinity of the solid substrate. As a result, a non-uniform and non-symmetric membrane tension builds up. It triggers lipid flow towards the regions of highest tension, in analogy to Marangoni flow. The gradients in the tension are strongest in the regions facing the electrodes. There the membrane starts flowing downwards. At the bottom of the vesicle, where two oppositely directed flows meet, the membrane material is pushed upward along the equator for reasons of mass conservation. At the top, the flow splits in two directions downwards to the two poles due to gravity. These are the principal flow lines as sketched in Fig. 1f for a field frequency up to 1 MHz. Interestingly, the frequency at which we observe reversal of the flow direction, *i.e.* around 3 MHz, coincides with the Maxwell–Wagner frequency, above which the polarization of the vesicle is determined by the media permittivities. Thus, the reversal of the flow direction may be due to the difference between the permittivities of the glucose and the sucrose solutions. The flow in the membrane is expected to induce fluid motion in the inner and

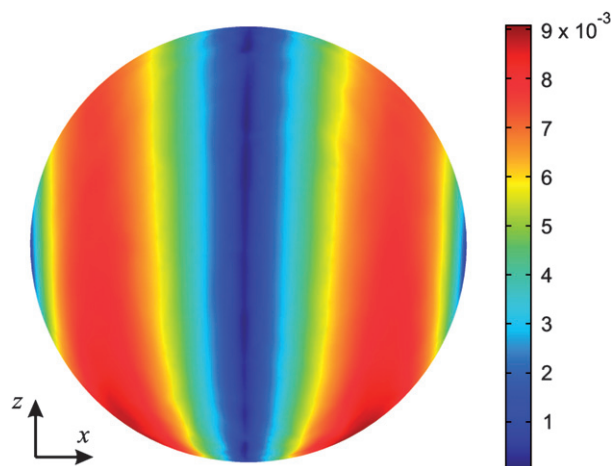


**Fig. 3** Lateral electric stress magnitude on the surface of a vesicle as defined in the text (for parameters see Fig. 2). The applied electric field is directed along the  $x$  axis. The calculated values of the stress have been divided by  $\epsilon_{\text{ex}}E_0^2$  corresponding to a homogeneous electric field  $E_0$  acting on a homogeneous external medium with dielectric constant  $\epsilon_{\text{ex}}$ .

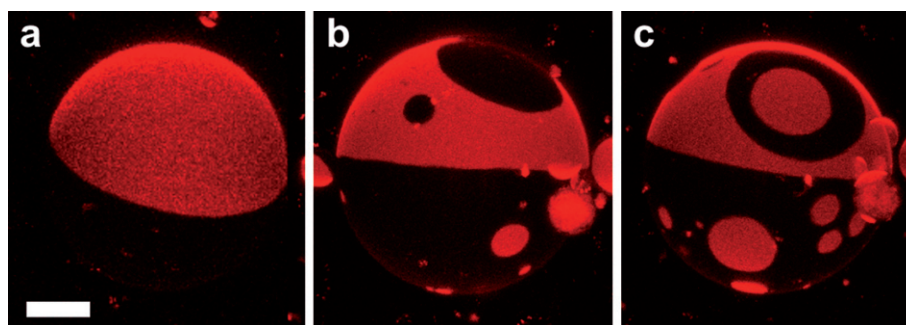


**Fig. 4** 3D confocal scans of the lower vesicle hemisphere illustrating lipid mixing induced by AC field (80 kHz,  $500 \text{ V cm}^{-1}$ ), at an external conductivity of  $250 \mu\text{S cm}^{-1}$ . The vesicle ( $\sim 95 \mu\text{m}$  diameter) was prepared from a mixture of 2.66 : 5.33 : 2 DOPC : DPPC : Chol. Before applying the field (a), the vesicle has only two domains, which break apart after continuous field exposure of 2 min (b) and 3 min (c). The scale bar corresponds to  $25 \mu\text{m}$ .

outer media, *via* viscous coupling, but we did not attempt to visualize it.

The above mechanism is only an initial conjecture explaining the observed lipid flow lines based on the numerical calculations of the electric field and lateral stress. It does not account for possible hydrodynamic effects and shielding from neighbour vesicles.

The AC field-induced membrane flow may possibly find significant application in microfluidic technologies. Giant vesicles in inhomogeneous AC fields or in hydrodynamic flows mimicking, *e.g.*, the situation of red blood cells in capillaries may be used as nano-reactors for fluid manipulation, *i.e.* displacing, mixing, trapping, *etc.* To demonstrate lipid mixing, we performed experiments where lipid vesicles composed of only one  $I_o$  and one  $I_d$  domain, are exposed to an AC field for a certain period of time. One example is shown in Fig. 4. The field-induced membrane flow causes domain fission leading to the appearance of a large number of smaller domains; see also the movies in the ESI.† In a fission process, there is a competition between the domain line tension and the local lateral force on the membrane. Therefore, for low field strengths or low external salt concentrations, the lateral stress is insufficient to overcome the line tension, and the domains only deform. For sufficiently strong membrane flows, the number of domains grows with the time of exposure. This, on the other hand, increases the probability of domain encounter and fusion. Domain fusion counterbalances the fission and therefore, after a certain time, the domains will reach a stationary state characterized by a certain size distribution. Since the membrane flow follows a certain pattern, the lipid mixing is not random. Domain fusion and fission are observed only at the bottom part of the vesicle, where oppositely directed flows meet and are deflected. At the stagnation points in the centres of the circular trajectories (see Fig. 1f) the membrane material may be trapped and a certain quasi-stable domain configuration surrounded by fast flowing domains may be observed (Fig. 4c). After switching the field off, the domains are not in equilibrium and slowly fuse back into two big domains.

The AC field-induced lipid flow as demonstrated here for giant vesicles with intramembrane domains opens a new direction of research. Such membrane labelling allows visualization of lipid displacement and we believe that this approach will be helpful for studies on membrane behaviour in vesicles subjected to shear flows<sup>13</sup>

or mechanical stresses. Investigating electric field-induced membrane flows may also lead to a deeper understanding of a widely used but poorly understood technique for giant vesicle preparation, namely the electroformation method.<sup>9</sup> Finally, we expect to observe other interesting electro-osmotic phenomena by studying the influence of the electric field geometry and the shape of the vesicle on the flow pattern.

## Acknowledgements

MS thanks N. Bezlyepkina, R. Knorr, S. Aranda and Y. Li for experimental support. We acknowledge P. Vlahovska for fruitful discussions and critical reading of the text.

## Notes and references

- 1 T. M. Squires and M. Z. Bazant, *J. Fluid. Mech.*, 2004, **509**, 217–252.
- 2 (a) H. Schwan, *Blut*, 1983, **46**, 185–197; (b) J. Yang, Y. Huang, X. Wang, X-B. Wang, F. Becker and P. Gascoyne, *Biophys. J.*, 1999, **76**, 3307–3314; (c) R. Dimova, K. Riske, S. Aranda, N. Bezlyepkina, R. Knorr and R. Lipowsky, *Soft Matter*, 2007, **3**, 817–927.
- 3 (a) U. Zimmermann, *Electromanipulation of Cells*, CRC Press, Boca Raton, FL, 1996; (b) J. Voldman, *Annu. Rev. Biomed. Eng.*, 2006, **8**, 425–454.
- 4 G. I. Taylor, *Proc. R. Soc. London, Ser. A*, 1966, **291**, 159–166.
- 5 (a) V. A. Murtsovkin, *Colloid J. (Transl. of Kolloidn. Zh.)*, 1996, **58**, 341–349; (b) G. Yossifon, I. Frankel and T. Miloh, *Phys. Fluids*, 2007, **19**, 068105.
- 6 (a) A. Ramos, H. Morgan, N. G. Green and A. Castellanos, *J. Colloid Interface Sci.*, 1999, **217**, 420–422; (b) M. Z. Bazant and T. M. Squires, *Phys. Rev. Lett.*, 2004, **92**, 066101.
- 7 (a) W. Helfrich, *Z. Naturforsch.*, 1973, **29c**, 693–703; (b) H. Hyuga, K. Kinoshita and N. Wakabayashi, *Jpn. J. Appl. Phys.*, 1991, **30**, 2649–2656.
- 8 S. Lecuyer, W. Ristenpart, O. Vincent and H. Stone, *Appl. Phys. Lett.*, 2008, **92**, 104105.
- 9 M. Angelova and D. Dimitrov, *Faraday Discuss. Chem. Soc.*, 1986, **81**, 303–311.
- 10 S. Veatch and S. Keller, *Phys. Rev. Lett.*, 2002, **89**, 268101.
- 11 S. Aranda, K. Riske, R. Lipowsky and R. Dimova, *Biophys. J.*, 2008, **95**, L19–L21.
- 12 H. Pauly and H. Schwan, *Z. Naturforsch.*, 1959, **14b**, 125–131.
- 13 (a) C. Vézý, G. Massiera and A. Viallat, *Soft Matter*, 2007, **3**, 844–851; (b) M. Abkarian and A. Viallat, *Soft Matter*, 2008, **4**, 653–657.

# Membrane flow patterns in multicomponent giant vesicles induced by alternating electric fields

Margarita Staykova, Reinhard Lipowsky and Rumiana Dimova\*

*Max Planck Institute of Colloids and Interfaces, Science Park Golm, 14424 Potsdam, Germany*

## Supplementary information

### 1. Preparation of giant lipid vesicles (GUVs):

GUVs were prepared using the electroformation method, introduced by Angelova and Dimitrov.<sup>1</sup> Stock solutions of 4 mM lipid in chloroform were prepared from dioleoylphosphatidylcholine (DOPC), dipalmitoylphosphatidylcholine (DPPC) and cholesterol (Chol), and subsequently mixed to form solutions with 5.33:2.66:2, 2.665.3:3:2 and 4.8:3.2:2 DOPC:DPPC:Chol molar lipid ratios. The fluorescent dye N-(lyssamine rhodamine B sulphonyl)-dipalmitoylphosphatidylethanolamine (Rh-DPPE) was added to the mixture (0.1 mol %). A small volume (12  $\mu$ l) of the lipid solution was spread on the conductive surfaces of two glass plates coated with indium tin oxide. The latter were kept at around 60°C and under vacuum for approximately 2 h to remove all traces of the organic solvent. The two glasses were placed with their conductive sides facing each other and separated by a 2 mm-thick Teflon frame to form a chamber, which was sealed with silicon grease. The chamber was then gently filled with preheated sucrose solution (0.01 to 0.1 M) and placed in an oven at 60°C. The glass plates were connected to a function generator and an alternating current (700 mV, 10 Hz frequency) was applied for one hour. Vesicles with an average diameter of 50  $\mu$ m and a large polydispersity were observed after about 2 hours. Then, a 5 Hz current of 2 V was applied for another hour to detach the vesicles from the glass surfaces. The vesicle solution was let to cool slowly, removed from the electroswelling chamber and diluted 40 times into an isotonic glucose solution. The osmolarities of the sucrose and glucose solutions were measured with cryoscopic osmometer Osmomat 030 (Gonotec, Berlin, Germany) and carefully matched to avoid an osmotic pressure difference. The conductivity of the glucose solution was adjusted by adding NaCl solution and measured with conductivity meter SevenEasy (Mettler Toledo, Greifensee, Switzerland).

Approximately 1 ml of the obtained vesicle solution was placed in a chamber for electromanipulation purchased from Eppendorf (Hamburg, Germany). Because of the differences in density and refractive index between the sucrose and glucose solutions, the vesicles were stabilized by gravity at the bottom of the chamber.

At room temperature, lipid membranes with the above composition are in the two-phase coexistence region.<sup>2</sup> The vesicles exhibit liquid ordered ( $l_o$ ) and liquid disordered ( $l_d$ ) domains. Rh-DPPE is known to partition in the  $l_d$  phase.<sup>3</sup> After equilibration, the vesicles typically contained one  $l_o$  domain and one  $l_d$  domain. We preheated them to obtain a larger number of smaller domains before subjecting them to electric fields.

### 2. Supplementary movie material

All movies were recorded with an inverted confocal laser scanning microscope Leica DM IRE2 (Leica Microsystems Heidelberg GmbH, Germany) using 40 $\times$  Ph2 objective and laser excitation at 561 nm (DPSS laser). Emission light was detected by a photomultiplier tube in the spectral range 580- 650 nm. The  $l_d$  domains are stained in red by Rh-DPPE, whereas the  $l_o$  ones appear black. The direction of the field is the same in all movies and is denoted by an arrow.

**Movie 1** Flow pattern in the lower part of a vesicle: The vesicle corresponds to the one in Fig. 1 in the article. The applied AC field is 360 V/cm, 80 kHz. The vesicle was prepared from 4.8:3.2:2 DOPC:DPPC:Chol solution. The conductivity of the external medium is 250  $\mu$ S/cm. The vesicle diameter is 150  $\mu$ m. The domains move from the polar regions (see Fig. 1 in the article) towards the lowest point of the vesicle (the middle of the image) and then towards the equatorial region. Domain fission can be also observed. The movie is speeded up 4.2 times.

**Movie 2** Flow pattern in the upper part of a vesicle: This movie is recorded at the same exposure conditions as Movie 1 and for the same vesicle. The flow at the top part of the vesicle is in opposite direction and slower than the flow at the bottom part (Movie 1). The movie is speeded up 4.2 times.

**Movie 3** Frequency dependence of the flow in the lower part of the vesicle: The vesicle was prepared from 5.33:2.66:2 DOPC:DPPC:Chol solution. An AC field at a fixed strength of 260 V/cm and for three different frequencies (500 kHz, 1 MHz and 3 MHz) was applied. The conductivity of the external medium is 360  $\mu$ S/cm and the diameter of the vesicle is approximately 120  $\mu$ m. For the low frequency (500 KHz), the direction of the membrane flow is as described in Movie 1. At 1 MHz the flow almost ceases and at 3 MHz its direction reverses. Between the field frequency switches, the vesicle is not exposed to an AC field. The movie is speeded up 8.4 times.

**Movie 4** AC-field induced lipid mixing: The movie shows the bottom part of a vesicle (180  $\mu$ m in diameter) that has been prepared from 2.665.3:3:2 DOPC:DPPC:Chol. Such membrane composition favors lipid segregation in

two large domains –  $l_d$ , stained in red and  $l_o$ , in black. At the beginning of the movie, before the field application, the bottom part of the vesicle is occupied mainly by the red  $l_d$  domain. The membrane on the upper part of the vesicle is in the  $l_o$  phase (dark). The small black domains in the red  $l_d$  phase are due to mixing from previous exposures to electric field. The AC field exposure (500 V/cm, 80 kHz) at an external conductivity of 250  $\mu$ S/cm causes a strong membrane flow, observed as dark protrusions of the  $l_o$  phase in the red  $l_d$  phase. The movie is speeded up 4.2 times.

### 3. Numerical simulations

The calculations were done in 3D and in the quasi-static approximation, using the commercially available modeling package COMSOL (Multiphysics, Germany). The parameters for the calculations, as given in Table 1, matched the experimental conditions.

Parameter name	Symbol notation	Value	Units
Internal dielectric constant	$\epsilon_{in}$	$7.08 \times 10^{-10}$	$C^2 J^{-1} m^{-1}$
External dielectric constant	$\epsilon_{ex}$	$7.08 \times 10^{-10}$	$C^2 J^{-1} m^{-1}$
Membrane dielectric constant	$\epsilon_{me}$	$2.66 \times 10^{-11}$	$C^2 J^{-1} m^{-1}$
Internal electric conductivity	$\lambda_{in}$	$3 \times 10^{-4}$	$S m^{-1}$
External electric conductivity	$\lambda_{ex}$	$3 \times 10^{-2}$	$S m^{-1}$
Membrane electric conductivity	$\lambda_{me}$	$10 \times 10^{-10}$	$S m^{-1}$
External vesicle radius	$R$	$40 \times 10^{-6}$	m
Membrane thickness	$d$	$5 \times 10^{-9}$	m
Angular frequency	$\omega$	$628 \times 10^3$	$Rad s^{-1}$

**Table 1** Parameters used for the numerical calculations.

#### 3.1. Dielectric model

Lipid vesicles are commonly modeled as single shell objects with confocal geometry, i.e., the two surfaces bounding the shell are ellipsoids with the same foci. The internal vesicle solution, the membrane and the external medium are leaky dielectrics defined by complex permittivity ( $\epsilon$ ), which comprises the influence of both their electric conductivity and dielectric permittivity:

$$\epsilon_k = \sigma_k + i\omega\epsilon_k \quad , \quad \text{with } k = in, me, \text{ and } ex,$$

where  $i$  is the imaginary number (see Table 1 for symbol definition).

The single shell model can be further simplified using the Maxwell body approximation, according to which, any spherical confocal single shell object may be represented as a homogenous sphere of the same external radius ( $R$ ), having an effective permittivity ( $\epsilon_{eff}$ ) and the same polarization as the one of the shell (Fig. 1S). The effective permittivity of the equivalent body is given by:<sup>4</sup>

$$\epsilon_{eff} = \epsilon_{me} \frac{2(1-\nu)\epsilon_{me} + (1+2\nu)\epsilon_{in}}{(2+\nu)\epsilon_{me} + (1-\nu)\epsilon_{in}}, \quad \text{where } \nu = (1-d/R)^3 \text{ is a geometric factor and } d \text{ is the membrane thickness.}$$

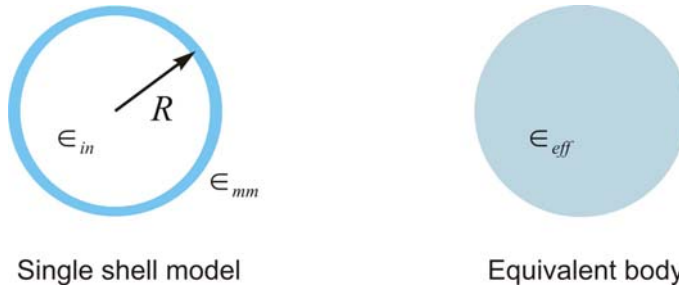


**Fig. 1S.** Schematic illustration of dielectric models of a lipid vesicle.

The electric potential is a solution of the Laplace equation. The normal component of the electric current density across the vesicle interface is continuous, whereas at the external boundaries, i.e. the box walls, it is zero (insulators). The external field is generated between two cylindrical electrodes with voltages of 1 and -1 V at their boundaries.

### 3.2. Lateral electric stress for a vesicle in a homogeneous AC field.

As a test case, the lateral stress induced on the surface of a vesicle was calculated for a homogeneous electric field (Fig. 2S). The parameters for the calculation (field conditions, media properties, vesicle size) are analogous to the parameters used to obtain Fig. 3 in the article. The only difference is that the electrodes are far from any solid substrate and the vesicle is situated in the middle between them, i.e. it is subject to a homogenous AC field.

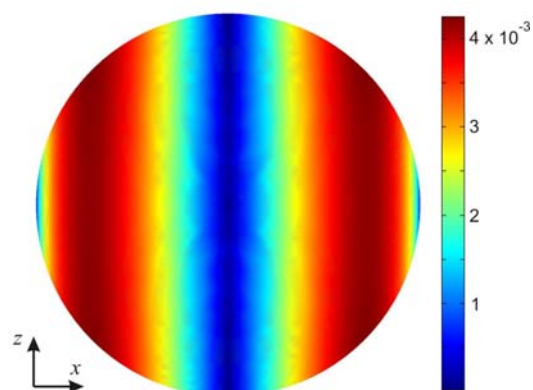


**Fig. 2S.** Lateral stress distribution on a vesicle in homogeneous AC field.

The numerical results show axially symmetric distribution of the lateral electric stress on the surface of the vesicle with maxima at  $\theta = \pm\pi/4$ , similar to results reported in the literature.<sup>5</sup> The symmetry axis is provided by the field direction. Note that the same stress distribution is observed also in droplets.<sup>6</sup> However, since the molecules at the droplet surface are not bound to the interface but are free to flow in the droplet interior, such stress distribution gives rise to a toroidal flow inside (as well as outside) as sketched in Fig. 3S. In vesicles, the lipids are bound to the vesicle surface. For an axially symmetric stress distribution (Fig. 2S), the gradient in the membrane tension on one side of the vesicle (e.g. the lower part) would be exactly balanced by identical gradient on the other (upper) side of the vesicle. Thus, no flow in the membrane is initiated. Note that in inhomogeneous fields, this balance is broken (see Fig. 3 in the article) giving rise to the flow described in the article.

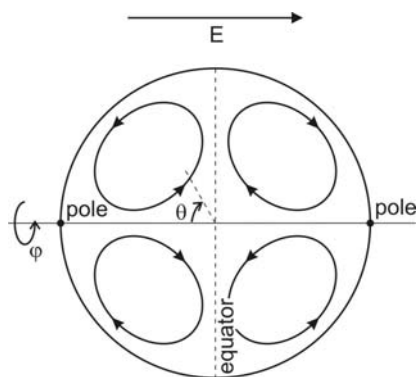


**Fig. 3S.** Sketch of the toroidal flow inside droplets subjected to homogeneous AC fields. The system has rotational symmetry along the azimuthal angle  $\varphi$ .

It is interesting to draw a parallel between the stress distribution on membranes in homogeneous electric fields and the concentration gradients observed in supported lipid bilayer. In the studies reporting the latter<sup>7,8</sup>, the field is applied along the surface of the planar supported bilayer and concentration gradients of the fluorescent marker are observed. These gradients, however, do not illustrate the stress profile in the supported membrane and is thus of entirely different nature as compared to the stress gradients driving the domains in vesicles in inhomogeneous fields as reported here.

#### References:

- 1 M. Angelova, D. Dimitrov. *Faraday Discuss. Chem. Soc.*, 1986, **81**, 303-311.
- 2 S. Veatch, S. Keller, *Phys. Rev. Lett.*, 2002, **89**, 268101.
- 3 T. Baumgart, G. Hunt, E. Farkas, W. Webb and G. Feigenson, *Biochim. Biophys. Acta.*, 2007, **1768**, 2182-2194.
- 4 H. Pauly and H. Schwan, *Z. Naturforsch.* 1959, **14b**, 125-131.
- 5 G. Yossifon, I. Frankel and T. Miloh, *Phys. Fluids*, 2007, **19**, 068105.
- 6 G. I. Taylor, *Proc. Royal Soc. A*, 1966, **291**, 159-166.
- 7 J. T. Groves and S. G. Boxer, *Biophys. J.*, 1995, **69**, 1972-1975.
- 8 J. T. Groves, S. G. Boxer and H. M. McConnell, *Proc. Natl. Acad. Sci. USA.*, 1998, **95**, 935-938